

vation laws) this is exactly equivalent to the rules of Ref. 1. It is clear that the same rules enable one to calculate any of the higher-order Green's functions in terms of the mean occupation number.

ACKNOWLEDGMENT

This work was carried out during my stay at the

Rockefeller University. I would like to thank my colleagues there for their hospitality during my visit.

*At present on leave at the Rockefeller University, New York, N. Y.

†At present National Science Foundation Senior Post-doctoral Fellow.

¹R. Balian and C. De Dominicis, Nucl. Phys. **25**, 529 (1961); **27**, 294 (1961).

²T. D. Lee and C. N. Yang, Phys. Rev. **117**, 22 (1960).

³See, for example, J. M. Luttinger and J. C. Ward, Phys. Rev. **118**, 1417 (1960).

⁴This result may be found in N. Hugenholtz and L. Van Hove, Physica **24**, 363 (1958).

⁵This is because the relationship between connected and disconnected diagrams is exactly the same as for the case of the thermal average of $S(\beta)$, being dependent only on Wick's theorem.

⁶See, for example, L. D. Landau and E. M. Lifshitz, *Statistical Physics* (Pergamon Press, London, 1958), p. 154 ff.

⁷A. A. Abrikosov, L. P. Gorkov, and I. E. Dzyaloshinski, *Method of Quantum Field Theory in Statistical Physics* (Prentice-Hall, Inc., 1963), p. 103 ff.

PHYSICAL REVIEW

VOLUME 174, NUMBER 1

5 OCTOBER 1968

Phonon Spectrum of hcp He^4 †

V. J. Minkiewicz, T. A. Kitchens, F. P. Lipschultz,* R. Nathans, and G. Shirane

Brookhaven National Laboratory, Upton, New York

(Received 25 April 1968)

The phonon dispersion relation of the quantum crystal hcp He^4 has been studied for wave vectors along the $[10\bar{1}0]$ and $[0001]$ symmetry directions. Of the 10 branches of the spectrum along these directions, we have observed phonon groups from all but two, the $\text{TO}_\perp [10\bar{1}0]$ and $\text{LO} [0001]$. The LO and $\text{LA} [10\bar{1}0]$ branches are only partially complete. The experimental results have been compared with a calculation for the spectrum by Gillis, Koehler, and Werthamer; the agreement is found to be reasonable. The excitations are found to be well defined, except for the $\text{LO} [10\bar{1}0]$ branch, where we observe a wave-vector-dependent relaxation. The single crystals of helium used for the experiment were held at $1.03 \pm 0.09^\circ\text{K}$ and had a molar volume of $21.1 \pm 0.1 \text{ cm}^3$.

I. INTRODUCTION

A fundamental understanding of the dynamical properties of highly anharmonic crystals continues to be one of the most challenging problems in the physics of solids.¹⁻⁸ In recent years, the properties of these solids have been the subjects of a great deal of renewed theoretical interest.⁹⁻¹⁵ In particular, the crystalline forms of the isotopes of helium have been singled out to receive special attention because of their weak interatomic interaction and the small atomic mass of the helium atom.

The feature that makes these solids unique is the dominant role played by the zero-point motion, especially for large molar volumes. For example, in the solid forms of He^4 the motion is so large that the ratio of the root-mean-square amplitude of vibration to the nearest-neighbor distance is typically of the order of $\frac{1}{3}$, and as a result, the contribution made by the zero-point energy repre-

sents approximately 98% of the total energy of the crystal.¹⁶ This large zero-point motion has a number of interesting consequences: one, for example, is that liquid helium does not solidify under its own vapor pressure, even for temperatures down to absolute zero. To produce solid helium, an external pressure must be applied to the liquid. Another very important consequence with far-reaching implications is that, after the solid is formed, the crystal is much larger than could be expected from the interatomic potential determined by the physical properties of the gas. Because of the role played by the zero-point motion, these crystals have often been called "quantum crystals," and their properties have been described within the framework of the quantum theory of the many-body problem. Of course not all of the solids formed by helium are "quantum crystals"; solid helium at small molar volume (i. e., high pressure) is, to a large extent, a normal classical solid. In this paper, we present experimental results that have

been taken in the quantum region of the phase diagram of He⁴.

Insofar as the experimental results in this paper deal with dynamical properties (i. e., the phonon spectrum) of solid He⁴, we present a brief survey, though not an historical one, of the relevant theoretical progress that has been made to date concerning this particular problem.

De Wette and Nijboer¹⁷ have performed a classical calculation for the phonon spectrum of hcp He⁴, where the interatomic interaction potential was taken to be of the Lennard-Jones type. They found that the classical approach proved to be strikingly unsuccessful. For the range of motor volume that hcp He⁴ is known to have, the calculation produced imaginary phonon energies throughout the Brillouin zone. Theoretically the crystal is just too large to support phonons using a bare Lennard-Jones potential with the parameters of the potential being fixed by the properties of the gas. In effect, as pointed out by de Wette and Nijboer, the harmonic approximation, namely the expansion of the interaction potential to second order in small displacements from equilibrium, is itself inadequate. Intuitively, of course, we expect the solid to support phonons, at least for small wave vectors. Brenig,⁶ and Fredkin and Werthamer⁷ have shown this to be the case. In Brenig's work, the one phonon state was explicitly constructed as a linear superposition of particle-hole excitations, and the time-dependent Hartree-Fock approximation was used to show that the state propagates through the crystal. Fredkin and Werthamer, applying the time-dependent Hartree approximation along with linear response theory, identified the one-phonon state with an isolated singularity in the single-particle response function. It is important to note that in both approaches a power expansion of the interaction potential is not necessary, and the single-particle aspect of the problem has been emphasized. On the other hand, the problem of whether or not the excitation is well defined (i. e., are relaxation effects important?) has not yet been well resolved theoretically, and has been, so far, largely left to experiment.^{11, 18, 19}

It had been recognized for some time that short range or "dynamic" correlations would play a major role in determining the properties of solid helium by reducing the effect of the hard core of the Lennard-Jones potential. Nosanow⁸ introduced, *a priori*, the Jastrow factor

$$f(r) = e^{-Kv(r)} \quad (1)$$

to take account of these short-range correlations. While the choice of Eq. (1) to represent the correlations is arbitrary and probably constitutes the poorest approximation made in this calculation, it does have the distinct advantage of having both a reasonable behavior and a simple analytic form which could easily be introduced into a computer calculation for the properties of the crystal. In Eq. (1), $v(r)$ is the Lennard-Jones potential

$$v(r) = 4\epsilon [(\sigma/r)^{12} - (\sigma/r)^6]. \quad (2)$$

With Eq. (1), Nosanow improved upon previous Hartree calculations by using

$$\begin{aligned} \psi(\vec{r}_1, \dots, \vec{r}_n) \\ = \prod_{i=1}^N \phi(\vec{r}_i - \vec{R}_i) \prod_{i < j \leq N} f(\vec{r}_j - \vec{r}_i) \end{aligned} \quad (3)$$

as the trial wave function in a variational calculation, where the ground-state energy had been calculated with a truncated cluster expansion. The approximation introduced by truncating the expansion has been considered by Hetherington *et al.*,²⁰ and more recently by Hansen and Levesque,²¹ who compare their "exact results" of a Monte Carlo calculation for the ground-state energy with the results obtained by Nosanow⁸ using the cluster expansion. They conclude that the expansion, using the trial wave function given by Eq. (3), converges nicely for solid helium. In Eq. (3),

$$\prod_{i=1, N} \phi(\vec{r}_i - \vec{R}_i)$$

is just the Hartree trial wave function, where $\phi(\vec{r}_i - \vec{R}_i)$ are the single-particle wave functions localized on lattice sites \vec{R}_i . The parameter K in Eq. (1) was used to minimize the total energy. It should be mentioned that the wave functions $\phi_i(r)$ were found to be very well approximated by a Heitler-London wave function

$$\phi(\vec{r}) \propto e^{-A/r^2}, \quad (4)$$

where A is a parameter that depends on molar volume. Using this formalism, Nosanow and Nosanow *et al.*,²²⁻²⁵ in a series of papers, have been able to obtain reasonable agreement with experiment for the sound velocity, the lattice constant, and the ground-state pressure and compressibility. The final form of the theory suggests another interpretation. In effect, what had been done was a Hartree calculation with an *effective* interaction potential $V(r)$, where

$$V(r) = [v(r) + (\hbar^2 K/M) \nabla^2 v(r)] e^{-2Kv(r)}, \quad (5)$$

where M is the atomic mass.

The next step is to calculate the phonon spectrum of the crystal. To accomplish this, the results of the time-dependent Hartree calculation were used to obtain the eigenvalue equation governing the phonon energies and polarizations, which for $T = 0^\circ\text{K}$ is given by²⁵

$$\begin{aligned} E^2(\vec{q}) \vec{\xi}_\lambda(\vec{q}) &= \frac{\hbar^2}{M} \sum_{\vec{R}_i} (1 - e^{-i\vec{q} \cdot \vec{R}_i}) \\ &\quad \times (\partial^2 / \partial \vec{R}_i \partial \vec{R}_i) \\ &\quad \times \int d^3x d^3x' \psi^2(x) \psi^2(x') V(|\vec{x} - \vec{x}' + \vec{R}_i|) \cdot \vec{\xi}_\lambda(\vec{q}). \end{aligned} \quad (6)$$

In Eq. (6), $E(\vec{q})$ is the phonon energy with wave vector \vec{q} for the λ' th branch and $\vec{\epsilon}_{\lambda'}(\vec{q})$ is the phonon polarization vector. The appropriate generalization of Eq. (6) for $T \neq 0$ has been considered by Gillis and Werthamer.¹¹ One very important feature of Eq. (6) is that it is exactly the classical eigenvalue equation with the exception that

$$\int d^3x d^3x' \psi^2(x) \psi^2(x') V(|\vec{x} - \vec{x}' + \vec{R}_i|) \quad (7)$$

has replaced the bare Lennard-Jones potential. The net result, as far as the phonon energies are concerned, is that one introduces an interatomic interaction potential in the classical dynamical matrix that is suitably softened to reduce the effect of the hard core (via correlations), and then averages over the mean probability distribution of the two interacting atoms.

In the discussion given above, we have so far considered those theories that stress the single-particle aspect of the problem. From a different point of view, a number of authors^{9, 12} have independently formulated theories that immediately stress not the single-particle behavior, but rather the collective aspects of the motion; as a result, these theories are known as self-consistent phonon theories. Most recently, Koehler⁹ has developed a variational approach to the lattice dynamics of these crystals that yields an improved value for the ground-state energy. Briefly, the gist of the method is to find a fictitious harmonic Hamiltonian that best approximates the true Hamiltonian of the crystal. The ground-state wave function is assumed to be

$$\prod_{i>j} f(\vec{r}_i - \vec{r}_j) \psi_0,$$

where ψ_0 is a correlated Gaussian.

$$\psi_0 \propto \exp - \frac{1}{2} \sum_{i,j} (\vec{r}_i - \vec{R}_i) \cdot \underline{G}_{ij} \cdot (\vec{r}_j - \vec{R}_j) \quad (8)$$

and $f(r)$ is a weight function taken to be of the form given by Eq. (1). The weight function $f(r)$ is introduced to account for short-range correlation, while the elements of the matrix \underline{G}_{ij} , which are related to the elements of the dynamical matrix, are determined variationally. Once again, the equation that determines the phonon energies is analogous to Eq. (6), but with the important difference that instead of averaging with the single particle distributions, an average is taken with respect to the harmonic phonon ground state. In this way, the calculation for the phonon energy becomes a self-consistent one. We should also mention that several authors, in particular Horner,¹⁰ using diagrammatic techniques, have produced results that in lowest order are equivalent to the self-consistent theories.

In this paper, the experimental results will be compared with a self-consistent calculation for the spectrum that has been performed by Gillis, Koehler, and Werthamer.²⁶ Part of the results of this work have been reported previously.²⁷ Polycrystalline specimens have been studied by Bitter *et al.* at 125 atm.²⁸

II. THE CRYOSTAT AND CRYSTAL GROWTH

The Cryostat

A special cryostat has been assembled for neutron scattering experiments on solid helium which allows for simultaneous measurement of the velocity of ultrasonic sound. The principal features of this cryostat are (1) low-neutron background, (2) *long-term* temperature and pressure stability, (3) the ability to orient the cryostat, and (4) the ability to grow large single crystals at low density.

The cryostat is schematically illustrated in Fig. 1. (The outside shell and the liquid-nitrogen shield and reservoir have been deleted for clarity.) The neutron background was minimized by using alumi-

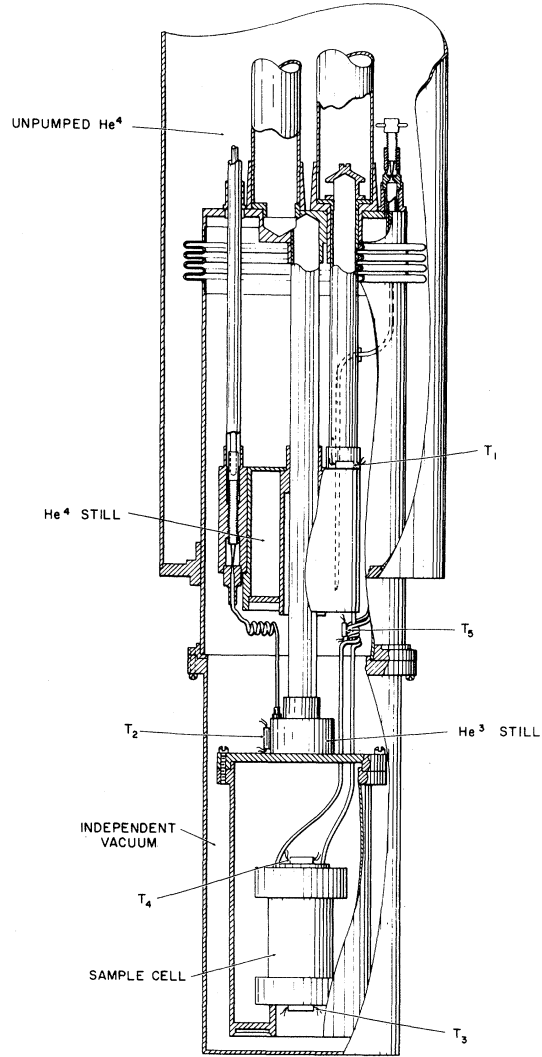


FIG. 1. A diagram of the recirculating He³ cryostat that was used for the experiment. The inside diameter of the sample chamber is 1 in.

num for all surfaces in the beam path and by demanding that the surfaces be as far away from the sample area as possible. The one exception to this rule is the sample chamber itself, which is constructed of No. 304 stainless steel with a wall thickness of 0.020 in. Experiment has shown that the background scattering from the chamber walls was temperature-independent.

The very important problem of long-term temperature stability was solved by using two separately pumped helium reservoirs. The upper reservoir, with a volume of 90 cm³, is connected to the unpumped helium chamber via a special needle valve which is controlled from the top of the cryostat. This reservoir, the He⁴ still in Fig. 1, could be filled through the needle valve while being held at $T < 1.3^\circ\text{K}$. The second reservoir, the He³ still in Fig. 1, was filled through another needle valve which, as is seen in the figure, is in good thermal contact with the He⁴ still. The He³ still was part of a closed recirculating system using a special sealed Edwards ED-150 pump with 4 liters of He³. This system was charged with He³ for two reasons: (1) It has a higher vapor pressure than He⁴, and (2) the thermal shorts which would exist in the system if it were filled with superfluid He⁴ are eliminated.

Resistance thermometers, designated T_1 through T_5 , were used throughout the experiment. The temperature of the sample chamber could be regulated with heaters at the top and bottom of the chamber with T_3 or T_4 in the servo loop. For a given scan through a phonon group, temperature stability of $\pm 0.010^\circ\text{K}$ could be maintained by a judicious choice of the pumping speed and the He³ needle valve position. In fact the uncertainty quoted for the sample temperature reflects the reproducibility of the valve setting over several months of data collection. Pressure stability was obtained by two servo systems in which the feedback signal is the error signal from a model-141 Texas Instruments Precision Bourdon Tube Pressure Gauge. The Bourdon tube used was of stainless steel, gave a range of 70 atm., and allowed the pressure to be maintained easily within 0.01 atm. The first servo system regulated the pressure by changing the temperature around the ambient temperature of 100°K of a fixed volume which communicates with the sample volume. The second servo system simply changed the volume of a room-temperature space which communicates with the sample chamber. The first system has a larger dynamic range but a slower response than the second.

The cryostat, with the booster pumps for the He³ and He⁴ stills, was mounted on a heavy-duty goniometer. The entire assembly could rotate 360° and could be tilted $\pm 6^\circ$ on two perpendicular axes.

Crystal Growth

The sample chamber used was designed to optimize the neutron scattering part of this experiment rather than the crystal-growing part of this experiment. It was, however, anticipated that large single crystals could be grown from the superfluid phase of He⁴ in spite of the awkward size, shape, and material of the chamber. Be-

cause of the very large thermal transport in the superfluid, any thermal gradients are suppressed, thereby inhibiting the formation of supercooled regions and new seed crystals.

The samples were grown from high-purity helium gas which was first passed through a liquid-helium cold trap and then admitted to the growing chamber through a capillary. The pressure in the cell was measured via a second capillary. The chamber was filled with liquid at ~ 25 atm, with heat being continually applied near thermometer T_5 to keep the capillaries unblocked. The pressure was then increased and the melting curve usually intersected at $T \cong 1.28^\circ\text{K}$. Pressure stability was maintained either by the servo mechanisms or by manually adjusting the mass flow to the chamber. Heat was removed from the bottom of the chamber by pumping on the He³. The temperature of the bottom (T_3) was observed to decrease while T_4 remained constant at the melting curve, confirming the fact that the thermal gradient was entirely in the solid forming at the bottom. When the chamber was filled with solid, the total growing time normally being about 1 h, T_3 and T_4 were observed to cool precipitously. The capillary heater was turned off and an excess pressure of 6 atm applied to eliminate the thermal short between the 4.2°K helium and the sample via superfluid He⁴ in the capillaries. Thus the periodic refilling of the He⁴ still was not at all critical.

No attempt was made to "seed" or grow crystals on a substrate, since several orientations were desired. In fact, in an attempt to obtain particular orientations, a few samples were deliberately "crushed" by slightly melting the top of the sample to allow an excess mass to rush into the chamber. A crystal oriented in a $[010]$ zone²⁹ was obtained in this manner. We should mention that in a few cases when careful growths were attempted, it was often observed that a large crystal was found *only after* about 36 h had passed, even when the sample was held at 1.0°K . On the other hand, the Bragg intensity of a reflection from the crystal, once it was located, did not vary significantly with time.

Data have been collected on six crystals, their mosaic spread being typically $9'$ (full width at half-maximum). The size of the crystals varied somewhat; a nominal size of ~ 1.0 cm³ was estimated by beam-masking experiments. The samples were held at $T = 1.03 \pm 0.09^\circ\text{K}$; the lattice parameters were found to be $a = 3.671 \pm 0.008 \text{ \AA}$ and $c = 6.012 \pm 0.008 \text{ \AA}$, which agree quite well with extrapolated values of neutron and x-ray measurements.³⁰ The molar volume of the crystals was therefore 21.1 ± 0.1 cm³. The errors that have been quoted for the temperature and molar volume were assigned by assuming that they should span the range of the parameters of the six different crystals that were used during the experiment.

III. EXPERIMENTAL TECHNIQUE

A total of 10 branches of the phonon spectrum of hep He⁴ can be studied for wave vectors along the $[100]$ and $[0001]$ principal symmetry directions; an incident neutron energy of 13.5 meV was used

throughout the experiment. We have observed phonon groups from all but two branches of the spectrum, the LO [0001] and TO_⊥ [10 $\bar{1}$ 0]. Here, because of the large energy transfers involved, the measurements were severely restricted by intensity considerations. The LA and LO [10 $\bar{1}$ 0] branches are only partially complete for reasons that will be given in the next section.

We obtained crystals oriented in three zones: the [010], [01 $\bar{1}$], and the [001]. Figure 2 summarizes the zones of the crystals and the regions in reciprocal space that were used to measure the remaining branches. The TO_{||} branch was measured with the crystal in the [001] zone. It is, of course, not necessary to use an oriented crystal to measure the longitudinal branches. To measure them, we have at times used crystals for which we knew only the [10 $\bar{1}$ 0] or [0001] direction.

The regions in reciprocal space that were used to observe the phonon groups are somewhat unconventional, and so we present a short discussion of the unique experimental restrictions imposed by the Debye-Waller factor of crystalline He⁴ at small molar volume. The cross section for single phonon creation in a constant-"Q" scan is given by³¹

$$\sigma_j \propto (n_j + 1) e^{-2W} g_j^2(\vec{q}, \vec{\tau}) \quad (9)$$

per steradian per unit cell; g_j^2 is the inelastic structure factor for the j 'th branch and is given by

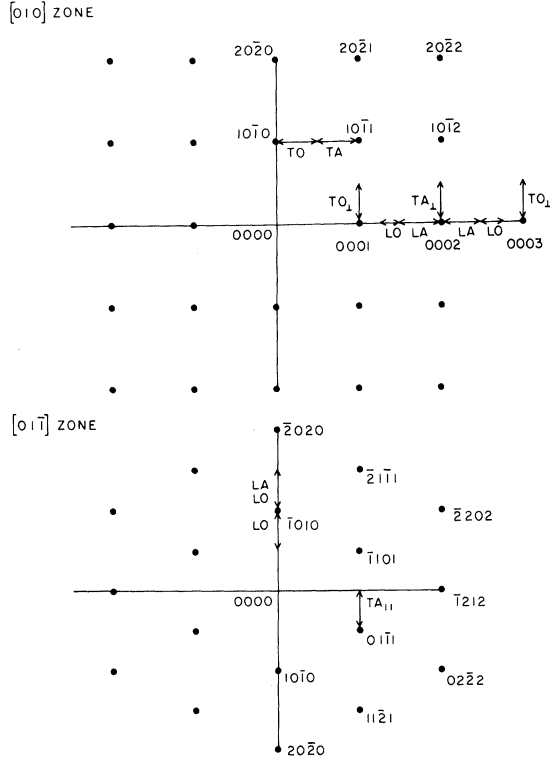


FIG. 2. The reciprocal lattice for the [010] and [01 $\bar{1}$] zones. The arrows represent the regions in reciprocal space, where the phonon spectrum has been studied.

$$g_j^2(\vec{q}, \vec{\tau}) = \left| \sum_k \frac{b \vec{Q} \cdot \vec{\xi}_{jk}(\vec{q})}{[ME_j(\vec{q})]^{1/2}} e^{i \vec{Q} \cdot \vec{\rho}_k} \right|^2 \quad (10)$$

where the sum is across the positions $\vec{\rho}_k$ of the atoms in the unit cell, n_j is the phonon occupation number, b and \vec{Q} are the coherent scattering length and scattering vector, respectively, and $2\pi\vec{\tau}$ is a reciprocal lattice vector. The familiar Debye-Waller factor is given by e^{-2W} , where in the Debye approximation

$$W = (3h^2/2Mk\theta)(Q/2\pi)^2 \quad (11)$$

for $T \ll \theta$, with θ the Debye temperature. Equation (11) represents that part of the Debye-Waller factor that is a result of the zero-point motion. While it is true that an isotropic Debye-Waller factor is not strictly correct for a solid such as hcp He, calculations have shown that the approximation should be reasonably accurate.²⁶ For He with $\theta = 25^\circ\text{K}$, $B = 3h^2/2Mk\theta \sim 29 \text{ \AA}^2$. This large value for B has a serious effect on the intensities of the phonon groups for He and should be compared with typical values for other materials, for example, $B_{\text{Na}}(\theta \sim 160^\circ\text{K}) = 0.78 \text{ \AA}^2$, $B_{\text{Ar}}(\theta \sim 93^\circ\text{K}) = 0.77 \text{ \AA}^2$, and $B_{\text{Ne}}(\theta \sim 75^\circ\text{K}) = 1.9 \text{ \AA}^2$.

For the hcp system, the structure factor usually dictates the optimum reciprocal lattice vector to be used for a particular branch. However, for the case of solid He, the large value for W effectively eliminates those with lengths greater than [10 $\bar{1}$ 0], [10 $\bar{1}$ 1], and [0002] reciprocal lattice vectors. One immediate consequence of being restricted to the first three reciprocal lattice vectors is to limit severely the intensity of the phonon groups via the factor $(\vec{Q} \cdot \vec{\xi})^2 e^{-2W}$ in Eq. (8); this is illustrated in Fig. 3, where we compare He, Ne, and Cu. In addition, for one branch of the spectrum, the Debye-Waller factor introduced another complication. Normally, the $TA_{||}$ [10 $\bar{1}$ 0] branch is measured with a crystal oriented in a [001] zone, and the data taken in the vicinity of the (2110) reflection. However, for the case of solid He, the Debye-Waller factor would dominate, and the phonon intensity would be severely reduced. In this case, a [01 $\bar{1}$] zone should be used, with the data collected around the (01 $\bar{1}$ 1) reflection, even though the observed phonon groups are somewhat contaminated by scattering from the TA_{\perp} [10 $\bar{1}$ 0] branch. The [01 $\bar{1}$] zone has the highest multiplicity in the hexagonal lattice. Finally, we compare the intensity of a "typical" phonon group that could be expected for solid He with Cu and Ne by evaluating Eq. (9) for "typical" experimental conditions; for He, Ne, and Cu, the intensities are in the ratio of 1:3.5:10 per unit volume.

The data reported in this paper were collected using a three-crystal neutron spectrometer operated in the constant-"Q" mode.³² Germanium crystals scattering from the (111) and (220) planes were used as the monochromator and analyzer, respectively. Since the visibility of a phonon group depends, to a large extent, on the ambient neutron background, a special effort was made to reduce the background to an acceptable level (< 1 count/min). Toward this

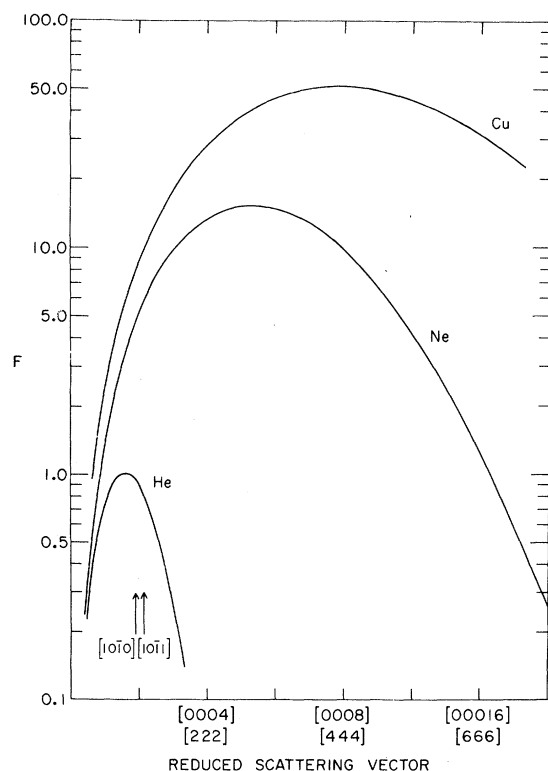


FIG. 3. The quantity $F = Q^2 e^{-2W}$ is plotted for hcp He^4 ($T = 1.0^\circ\text{K}$, $\theta \sim 25^\circ\text{K}$), Ne ($T = 4.2^\circ\text{K}$, $\theta \sim 75^\circ\text{K}$), and Cu ($T = 300^\circ\text{K}$, $\theta \sim 320^\circ\text{K}$). The scattering vector has been scaled to the [0002] reciprocal lattice vector for He and the [111] reciprocal lattice vector for Ne and Cu.

end, a pyrolytic graphite filter was used to reduce the high-energy component in the incident neutron beam. The samples were oriented by observing the Bragg scattering from the sample cell.

Before attempting to observe phonon groups from a particular sample, the cross section of the incident beam was reduced so as to match the size of the crystal of interest. This procedure does not eliminate all of the remaining solid helium in the beam path; however, the consistency of the data taken on different samples assures us that the phonon groups do not originate from extraneous crystals. As mentioned previously, we did not attempt to seed the crystals, and as a consequence, whether or not we obtained a suitably oriented crystal in a given growth cycle was a matter of chance. Normally, if we did not find an oriented crystal, the solid was immediately melted and a new growth begun.

IV. EXPERIMENTAL RESULTS AND DISCUSSION

Dispersion Relation

The phonon spectrum of the hexagonal phase of He^4 has been studied for wave vectors along the $[10\bar{1}0]$ and $[0001]$ principal symmetry directions exclusively. While it is possible to perform measurements for a general direction in the Brillouin zone, the added feature of the ambiguity of the phonon polarization

(i.e., the modes are neither purely transverse nor purely longitudinal) complicates their interpretation. On the other hand, the polarization vector of the modes along the principal symmetry directions can be strictly determined as being either one or the other. Over-all, the measurements have shown that the spectrum is quite normal. While at first this result may seem surprising in view of the nature of the solid, it is important to remember that the eigenvalue equation that determines the phonon dispersion relation is exactly the classical one (see Sec. I), which in turn is largely governed by purely geometrical factors. As long as the "averaged" interaction potential used in Eq. (6) is well behaved, the spectrum will appear likewise. A more detailed discussion of the phonon lifetime will be given in a later paragraph, but at this point we note that the surprising result of the experiment is that the excitations are as well defined as they are. Figure 4, for example, is a plot of some representative phonon profiles for various branches of the spectrum.

The final results of the measurements are listed in Tables I and II. The values quoted for the phonon energy and the errors assigned to them were obtained by the following procedure: The energy was determined by demanding that the integrated intensity on either side of the assigned peak position be equal, while the errors were calculated by a procedure given by Brockhouse *et al.*,³³ and then multiplied by two. The quoted errors, then, are twice the statistical error of the measurement; possible systematic errors have not been considered. In the case of a number of measurements being taken for the same phonon group, the appropriate statistical average has been taken. The data are plotted in Figs. 5, 6, and 7 along with the results

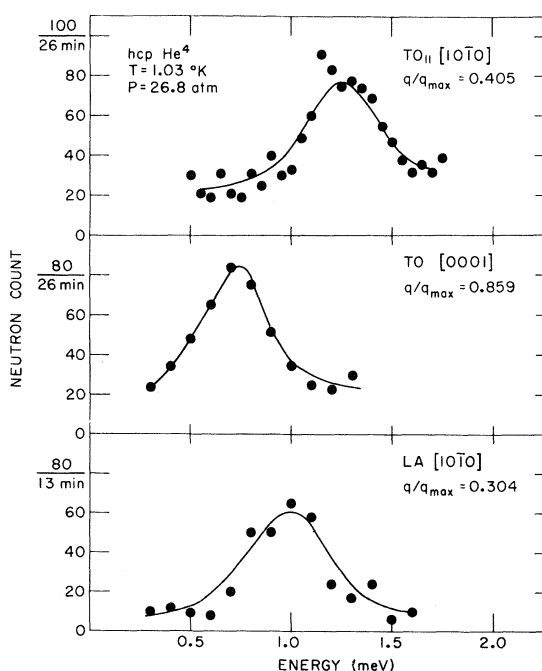


FIG. 4. Examples of some representative phonon group profiles for hcp He^4 .

TABLE I. Experimental results for the phonon spectrum of hcp He⁴ at 21.1 cm³/mole.

[10 $\bar{1}0$] LA		[10 $\bar{1}0$] LO	
q/q_{\max}	$E(\text{meV})$	q/q_{\max}	$E(\text{meV})$
0.101	0.31 ± 0.04	0.0	0.92 ± 0.02
0.152	0.45 ± 0.04	0.202	1.07 ± 0.03
0.202	0.65 ± 0.02	0.304	1.34 ± 0.08
0.253	0.76 ± 0.03	0.405	1.72 ± 0.07
0.304	0.99 ± 0.03	0.455	1.94 ± 0.16
0.405	1.21 ± 0.03	0.596	2.15 ± 0.12
0.455	1.42 ± 0.03	0.607	2.03 ± 0.14
0.506	1.54 ± 0.03		
0.556	1.62 ± 0.03		

[10 $\bar{1}0$] TA $_{\parallel}$		[10 $\bar{1}0$] TO $_{\parallel}$	
q/q_{\max}	$E(\text{meV})$	q/q_{\max}	$E(\text{meV})$
0.152	0.19 ± 0.05	0.101	1.03 ± 0.02
0.253	0.35 ± 0.03	0.202	0.94 ± 0.04
0.354	0.50 ± 0.03	0.304	1.12 ± 0.01
0.455	0.61 ± 0.04	0.405	1.24 ± 0.02
0.556	0.72 ± 0.04	0.506	1.35 ± 0.07
0.708	0.87 ± 0.01	0.658	1.51 ± 0.04
0.809	0.92 ± 0.03	0.809	1.56 ± 0.03
0.911	0.98 ± 0.02	0.911	1.69 ± 0.05
0.988	1.01 ± 0.03	1.000	1.63 ± 0.04

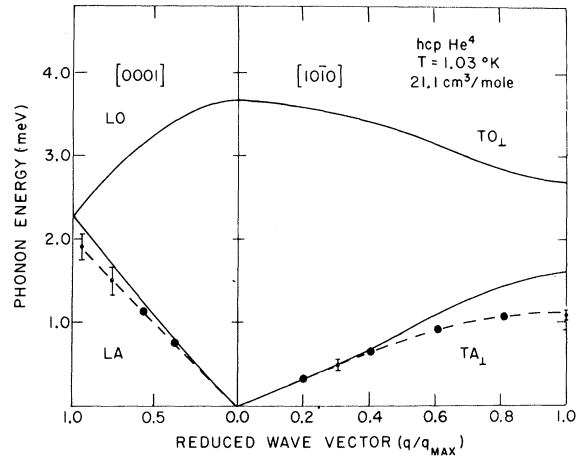
of the self-consistent calculation for the spectrum performed by Gillis, Koehler, and Werthamer.²⁶ In the calculation, the molar volume was fixed at 21.1 cm³.

The theoretical curves are generally higher than the experimental results. In connection with this point, Koehler³⁴ has compared the dispersion relation that he derives for bcc He³ with the spectrum obtained by Nosanow and Werthamer.²⁵ The result

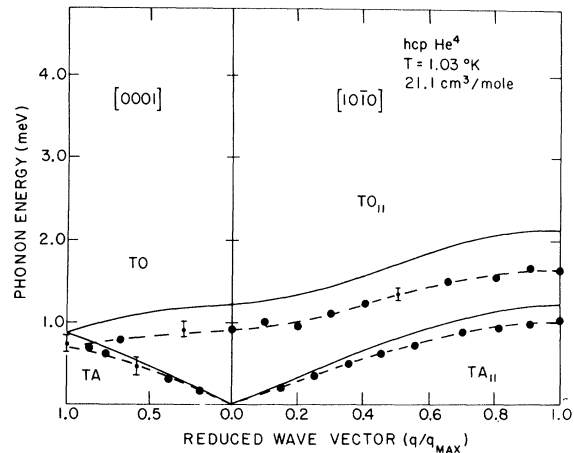
TABLE II. Experimental results for the phonon spectrum of hcp He⁴ at 21.1 cm³/mole.

[0001] TA		[0001] TO	
q/q_{\max}	$E(\text{meV})$	q/q_{\max}	$E(\text{meV})$
0.193	0.17 ± 0.03	0.285	0.92 ± 0.09
0.382	0.30 ± 0.04	0.669	0.78 ± 0.05
0.574	0.44 ± 0.14	0.859	0.69 ± 0.03
0.761	0.61 ± 0.06	0.989	0.74 ± 0.12

[0001] LA		[10 $\bar{1}0$] TA $_{\perp}$	
q/q_{\max}	$E(\text{meV})$	q/q_{\max}	$E(\text{meV})$
0.380	0.75 ± 0.04	0.202	0.35 ± 0.04
0.571	1.12 ± 0.05	0.304	0.49 ± 0.07
0.761	1.50 ± 0.17	0.405	0.67 ± 0.02
0.951	1.91 ± 0.15	0.607	0.91 ± 0.05
		0.809	1.10 ± 0.05
		1.000	1.08 ± 0.06

FIG. 5. The dispersion curves for the [10 $\bar{1}0$] TA $_{\perp}$ and the [0001] LA branches of the phonon spectrum for hcp He⁴. The solid lines are the theoretical results of Gillis, Koehler, and Werthamer.

is that the self-consistent phonon theory yields a crystal that is stiffer (the phonon energies are generally higher) than the one given by the "single-particle" theory. Gillis and Werthamer¹¹ have speculated that the correct theory will most likely be a judicious mixture of the self-consistent approach with those theories that emphasize the single-particle aspect of the problem. The agreement between experiment and theory can certainly be improved. However, considering that (a) the calculation is a first-principles one (i.e., there are no adjustable parameters, the length and energy scales of the Lennard-Jones potential having been fixed by the properties of the gas), (b) an approximation is made by introducing *a priori* the Jastrow factor to deal with the important problem of correlations, and (c) relaxation effects have been completely neglected, we feel that the agreement is reasonable at this stage.

FIG. 6. The dispersion curves for the [10 $\bar{1}0$] TA $_{\parallel}$ and TO $_{\parallel}$, and [0001] TA and TO branches of the phonon spectrum of hcp He⁴. The solid lines are the theoretical results of Gillis, Koehler, and Werthamer.

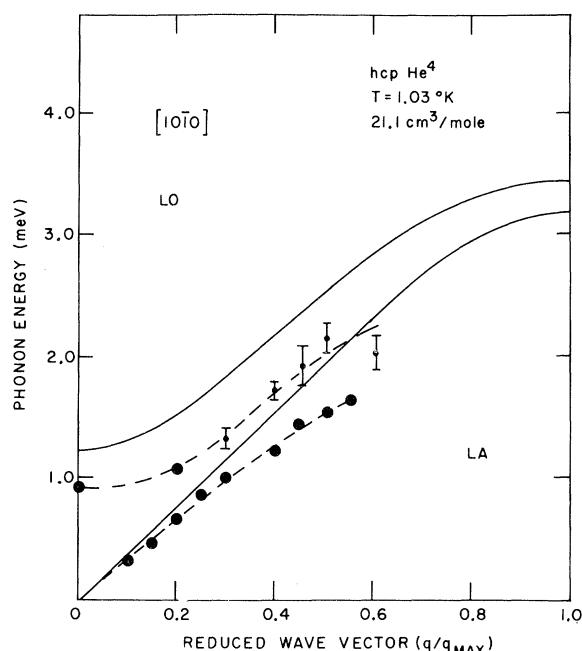


FIG. 7. The dispersion curves for the $[10\bar{1}0]$ LA and LO branches of the phonon spectrum for hcp He^4 . The solid lines are the theoretical results of Gillis, Koehler, and Werthamer.

Intensity and Linewidth

The intensity of the phonon groups for the LA $[10\bar{1}0]$ branch showed a strong wave-vector dependence; some representative groups for this branch are shown in Fig. 8. To determine whether the decrease in the intensity was, in fact, anomalous, we have used Eq. (9) to calculate its wave-vector dependence. The inelastic structure factor is, of course, model-dependent via $\xi_\lambda(\vec{q})$. However, we can expect that it would not be dependent in a sensitive way, and have therefore employed a model based on central forces that includes interactions to second nearest neighbors. This simple model does not reproduce the phonon spectrum. However, the calculation did show that while the variation of the Debye-Waller factor was approximately compensated for by the structure factor, the decrease in the intensity via $1/E(\vec{q})$ was found to be in qualitative agreement with experiment.

The determination of the intrinsic linewidth of a phonon mode using a three-crystal spectrometer is complicated by the fact that the observed group represents a convolution of the intrinsic (usually narrow) line profile of the excitation with the (usually wide) resolution function of the spectrometer. Cooper and Nathans³⁵ have recently developed a theory of the resolution properties of the spectrometer, and we use these calculations to estimate the intrinsic width. The results of computer calculations have shown that the experimental width of the phonon groups is largely due to the resolution of the spectrometer, with the exception of the LO $[10\bar{1}0]$ branch, where a definite wave-vector dependent broadening was observed. An upper

limit of ~ 0.09 -meV half-width at half-maximum (HWHM) could be set for the intrinsic width of the "normal" branches, while the linewidth of the LO $[10\bar{1}0]$ branch for $q/q_{\text{max}} \sim 0.5$ is estimated to be ~ 0.3 -meV (HWHM). Klemens¹⁹ has suggested that the three-phonon process could be the source of this rapid relaxation. Brun *et al.*³⁶ have observed similar relaxation effects for helium crystals with a molar volume of 16.03 cm^3 .

To summarize, the quantum crystal hcp He^4 has been shown to have, to a large extent, the normal phonon spectrum. The excitations are very well defined, except for the LO $[10\bar{1}0]$ branch well into the Brillouin zone, where we observe a wave-vector dependent broadening. Upon comparing the experimental spectrum with the results of the self-consistent phonon theory, we find that, while the agreement is reasonable, a great deal of improvement could be made.

Our studies of the phonon spectra in solid helium are being continued. Should efforts to grow larger single crystals of both the hcp and the bcc phase be successful, it will be possible to finish measuring the remaining branches in the hcp phase and to compare these results with similar data for lower molar volumes. Although the scattering experiment in the bcc phase is more straightforward, the cryogenic problems are considerably more serious.

ACKNOWLEDGMENTS

We want to express our gratitude to N. R. Werthamer, M. F. Collins, P. P. Craig, V. J. Emery,

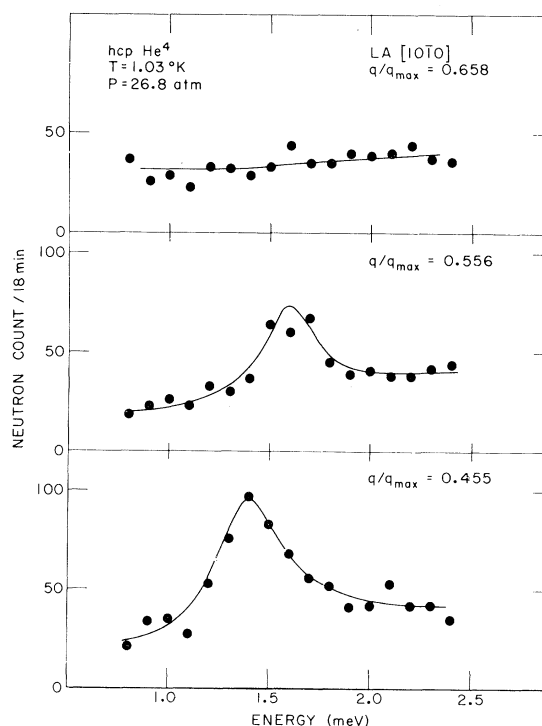


FIG. 8. Examples of the phonon group profiles for the $[10\bar{1}0]$ LA branch of the phonon spectrum of hcp He^4 .

P. G. Klemens, J. A. Leake, and L. H. Nosanow for many interesting and enlightening discussions during the course of this work. The expert techni-

cal assistance of T. Oversluizen and M. Rosso is also gratefully acknowledged.

[†]Work performed under the auspices of the U. S. Atomic Energy Commission.

*Present address: Physics Department and Institute of Materials Science, University of Connecticut, Storrs, Connecticut.

¹T. Nagamiya, Proc. Phys. Math. Soc. Japan **22**, 492 (1940).

²D. J. Hooton, Phil. Mag. **3**, 49 (1958).

³R. P. Hurst and J. M. H. Levelt, J. Chem. Phys. **34**, 54 (1961).

⁴N. Bernardes and H. Primakoff, Phys. Rev. **119**, 968 (1960).

⁵K. A. Brueckner and T. Froberg, in Many-Body Theory, edited by Ryugo Kubo (W. A. Benjamin, Inc., New York, 1966).

⁶W. Brenig, Z. Physik **171**, 60 (1963).

⁷D. R. Fredkin and N. R. Werthamer, Phys. Rev. **138**, A1527 (1965).

⁸L. H. Nosanow, Phys. Rev. **146**, 120 (1966).

⁹T. R. Koehler, Phys. Rev. **165**, 942 (1968).

¹⁰H. Horner, Z. Physik **205**, 72 (1967); G. Meissner, *ibid.* **205**, 249 (1967).

¹¹N. S. Gillis and N. R. Werthamer, Phys. Rev. **167**, 607 (1968).

¹²N. Boccara and G. Sarma, Physics **1**, 219 (1965).

¹³F. W. de Wette, L. H. Nosanow, and N. R. Werthamer, Phys. Rev. **162**, 824 (1968).

¹⁴W. J. Mullin, Phys. Rev. **166**, 142 (1968).

¹⁵J. Ranninger, Phys. Rev. **140**, A2031 (1965).

¹⁶J. Wilks, The Properties of Liquid and Solid Helium (Clarendon Press, Oxford, England, 1967).

¹⁷F. W. de Wette and B. R. A. Nijboer, Phys. Letters **18**, 19 (1965).

¹⁸C. C. Ackerman and R. A. Guyer, Solid State Commun. **5**, 671 (1967).

¹⁹P. G. Klemens, J. Appl. Phys. **38**, 4573 (1967).

²⁰J. H. Hetherington, W. J. Mullin, and L. H. Nosanow, Phys. Rev. **154**, 175 (1967).

²¹J. P. Hansen and D. Levesque, Phys. Rev. **165**, 293 (1968).

²²L. H. Nosanow and G. L. Shaw, Phys. Rev. **119**, 968 (1962).

²³L. H. Nosanow, Phys. Rev. Letters **13**, 270 (1964).

²⁴L. H. Nosanow and W. J. Mullin, Phys. Rev. Letters **14**, 133 (1965).

²⁵L. H. Nosanow and N. R. Werthamer, Phys. Rev. Letters **15**, 618 (1965).

²⁶N. S. Gillis, T. R. Koehler, and N. R. Werthamer, to be published. See also G. L. Morley, Ph. D. thesis, Iowa State University, 1967 (unpublished) for theoretical results at lower molar volumes of hcp helium using a similar formalism but neglecting dynamic correlations.

²⁷F. P. Lipschultz, V. J. Minkiewicz, T. A. Kitchens, G. Shirane, and R. Nathans, Phys. Rev. Letters **19**, 1307 (1967).

²⁸M. Bitter, W. Gissler, and T. Springer, Phys. Status Solidi **23**, K155 (1967).

²⁹The zone axis $[u, v, w]$ is defined by the relation $uh + vk + wl = 0$, where h , k , and l are the Miller indices of the reflections in the scattering plane.

³⁰W. H. Keesom and K. W. Taconis, Physica **5**, 161 (1938); D. G. Henshaw, Phys. Rev. **109**, 328 (1958); A. Schuch and R. Mills, Phys. Rev. Letters **8**, 469 (1962).

³¹B. N. Brockhouse and P. K. Iyengar, Phys. Rev. **111**, 747 (1958).

³²B. N. Brockhouse, in Inelastic Scattering of Neutrons in Solids and Liquids (International Atomic Energy Agency, Vienna, 1961) p. 113.

³³B. N. Brockhouse, T. Arase, G. Caglioti, K. R. Rao, and A. D. B. Woods, Phys. Rev. **128**, 1099 (1962).

³⁴T. R. Koehler, Phys. Rev. Letters **18**, 654 (1967).

³⁵M. J. Cooper and R. Nathans, Acta Cryst. **23**, 356 (1967).

³⁶T. O. Brun, S. K. Sinha, C. A. Swenson, and C. R. Tilford, to be published.